

Geophysical Research Letters®



RESEARCH LETTER

10.1029/2023GL103791

Radiative Forcing From the 2014–2022 Volcanic and Wildfire Injections

Key Points:

- Long-term balloon-borne measurements of stratospheric aerosol over Tibetan Plateau and U.S. are compared with an aerosol-climate model
- Stratospheric smoke particles generate 60% more negative effective radiative forcing than volcanic sulfate with the same aerosol optical depth
- Stratospheric aerosol abundance offsets 20% of the increase in the global mean surface temperature between 2014–2022 and 1999–2002

Supporting Information:

Supporting Information may be found in the online version of this article.

Correspondence to:

P. Yu,
pengfei.yu@colorado.edu

Citation:

Yu, P., Portmann, R. W., Peng, Y., Liu, C.-C., Zhu, Y., Asher, E., et al. (2023). Radiative forcing from the 2014–2022 volcanic and wildfire injections. *Geophysical Research Letters*, 50, e2023GL103791. <https://doi.org/10.1029/2023GL103791>

Received 21 MAR 2023

Accepted 15 JUN 2023

Author Contributions:








Conceptualization: Pengfei Yu, Michael Mills, Anja Schmidt, Karen H. Rosenlof, Owen B. Toon

Funding acquisition: Pengfei Yu
Investigation: Pengfei Yu, Robert W. Portmann, Yifeng Peng, Cheng-Cheng Liu, Michael Mills, Anja Schmidt, Owen B. Toon

Methodology: Pengfei Yu, Robert W. Portmann, Yunqian Zhu, Elizabeth Asher, Zhixuan Bai, Jianchun Bian, Michael Mills, Anja Schmidt

© 2023. The Authors.

This is an open access article under the terms of the [Creative Commons Attribution-NonCommercial-NoDerivs License](#), which permits use and distribution in any medium, provided the original work is properly cited, the use is non-commercial and no modifications or adaptations are made.

Pengfei Yu¹ , Robert W. Portmann² , Yifeng Peng³, Cheng-Cheng Liu⁴ , Yunqian Zhu^{2,5} , Elizabeth Asher^{2,6,7}, Zhixuan Bai⁸, Ye Lu^{8,9}, Jianchun Bian^{3,8,9} , Michael Mills¹⁰ , Anja Schmidt^{11,12,13}, Karen H. Rosenlof² , and Owen B. Toon^{5,14} 

¹Institute for Environmental and Climate Research, Jinan University, Guangzhou, China, ²Chemical Science Laboratory, National Oceanic and Atmospheric Administration, Boulder, CO, USA, ³College of Atmospheric Sciences, Lanzhou University, Lanzhou, China, ⁴School of Earth and Space Sciences, University of Science and Technology of China, Hefei, China, ⁵Laboratory of Atmospheric and Space Sciences, University of Colorado, Boulder, CO, USA, ⁶Cooperative Institute for Research in Environmental Sciences, University of Colorado, Boulder, CO, USA, ⁷Now at Global Monitoring Laboratory, National Oceanic and Atmospheric Administration, Boulder, CO, USA, ⁸Key Laboratory of Middle Atmosphere and Global Environment Observation, Institute of Atmospheric Physics, Chinese Academy of Science, Beijing, China, ⁹College of Earth and Planetary Sciences, University of Chinese Academy of Sciences, Beijing, China, ¹⁰Atmospheric Chemistry Observations & Modeling Lab, National Center for Atmospheric Research, Boulder, CO, USA, ¹¹German Aerospace Center (DLR), Institute of Atmospheric Physics (IPA), Weßling, Germany, ¹²Meteorological Institute, Ludwig Maximilian University of Munich, Munich, Germany, ¹³Yusuf Hamied Department of Chemistry, University of Cambridge, Cambridge, UK, ¹⁴Department of Atmospheric and Oceanic Sciences, University of Colorado, Boulder, CO, USA

Abstract Volcanic and wildfire events between 2014 and 2022 injected ~3.2 Tg of sulfur dioxide and 0.8 Tg of smoke aerosols into the stratosphere. With injections at higher altitudes and lower latitudes, the simulated stratospheric lifetime of the 2014–2022 injections is about 50% longer than the volcanic 2005–2013 injections. The simulated global mean effective radiative forcing (ERF) of 2014–2022 is -0.18 W m^{-2} , ~40% of the ERF of the period of 1991–1999 with a large-magnitude volcanic eruption (Pinatubo). Our climate model suggests that the stratospheric smoke aerosols generate ~60% more negative ERF than volcanic sulfate per unit aerosol optical depth. Studies that fail to account for the different radiative properties of wildfire smoke relative to volcanic sulfate will likely underestimate the negative stratospheric forcings. Our analysis suggests that stratospheric injections offset 20% of the increase in global mean surface temperature between 2014–2022 and 1999–2002.

Plain Language Summary Between 2014 and 2022, volcanic and wildfire events injected about ~3.2 Tg of sulfur dioxide and 0.8 Tg of smoke aerosols into the stratosphere, about 30%–40% of injected mass of the 1991 Pinatubo eruption. Because the sulfur dioxide and smoke aerosols are injected at higher altitudes and lower latitudes, the simulated aerosol lifetime is 50% longer than the volcanic injections between 2005 and 2013, which have been suggested to play a role in the global warming hiatus. Our climate model suggests that smoke aerosol generates 60% more negative effective radiative forcing compared with volcanic sulfate aerosol per unit change in aerosol optical depth. Our study underscores the distinct optical properties between the wildfire smoke and sulfate aerosol. Our analysis finds that the trend of the global mean surface temperature in the two decades would have been 24% larger without the stratospheric injections.

1. Introduction

Between 2014 and 2022, a number of volcanic eruptions and two extreme wildfire events injected a total of ~3.2 Tg of SO_2 and 0.8 Tg of smoke aerosols into the stratosphere. The injected mass is ~85% of that injected between 2005 and 2013, and ~40% of that injected in 1991 from the Mt. Pinatubo eruption. Stratospheric sulfate aerosols provide heterogeneous surfaces for N_2O_5 hydrolysis and reactions that release reactive halogen species (Solomon, 1999). The 2015 Calbuco volcanic eruption (41.3°S, 72.6°W) depleted the lower stratospheric ozone of the Antarctic and mid-latitudes by 30%–60% (Ivy et al., 2017; Solomon et al., 2016; Stone et al., 2017; Zhu et al., 2018). Recent satellite and modeling studies have shown that smoke aerosols provide surfaces for heterogeneous reactions that destroy ozone (Bernath et al., 2022; Santee et al., 2022; Solomon et al., 2022, 2023; Yu et al., 2021).

Project Administration: Pengfei Yu
Supervision: Pengfei Yu, Owen B. Toon
Visualization: Pengfei Yu, Yifeng Peng, Ye Lu
Writing – original draft: Pengfei Yu, Owen B. Toon
Writing – review & editing: Pengfei Yu, Robert W. Portmann, Yunqian Zhu, Elizabeth Asher, Michael Mills, Anja Schmidt, Karen H. Rosenlof, Owen B. Toon

The persistently variable stratospheric aerosol causes negative radiative forcing at the top of the atmosphere and partially offsets global warming, even in the absence of major volcanic eruptions (Solomon et al., 2011). Both volcanic sulfate and smoke aerosols exert a cooling by scattering sunlight back to space, but each has distinct radiative properties. Sulfate warms the stratosphere mainly through absorption of outgoing longwave radiation and solar radiation in the near infrared. In contrast, smoke aerosols, consisting mostly of organics and black carbon, absorb incoming solar radiation over a broad region of the solar spectrum and effectively warm the stratosphere (Rieger et al., 2021; Santee et al., 2022; Yu et al., 2021).

Here, we examine the effective radiative forcing of these injections relative to the volcanic quiescent period of 1999–2002 and the period of 2005–2013 when it has been suggested that moderate volcanic emissions partially offset the rate of increase of global temperature (Santer et al., 2014; A. Schmidt et al., 2018; G. A. Schmidt et al., 2014; Solomon et al., 2011). We conduct numerical simulations of the chemical and radiative effects of stratospheric aerosols. We compare the simulations with observational data on stratospheric aerosol abundance and use the simulations to compute the relative contribution to the global mean effective radiative forcings (ERF) by stratospheric volcanic and wildfire aerosols.

2. Methods

2.1. Emissions of Volcanoes and Wildfire Events

A number of volcanic eruptions perturbed the stratospheric chemistry and dynamics between 2014 and 2022. The volcanic emission database is described in previous studies (Mills et al., 2016; Neely III & Schmidt, 2016) and listed in Table S1 in Supporting Information S1. During 2014–2022, two major wildfire events perturbed the stratospheric chemistry and aerosol budget. One major event happened in the Pacific Northwest near 52°N (PNE fire) on August 12 of 2017, and the estimated particulate emissions were ~0.3 Tg of organics with 0.006 Tg of black carbon (BC) according to a modeling study (Yu et al., 2019). The other major event happened over several days around New Year's Eve 2020 in Australia near 40°S which we refer to as ANY fires. The fire plumes quickly rose to 12 km in a few hours to days, and the estimated emissions at 12 km were about 0.9 Tg of organics with 0.023 Tg of BC, about 3 times the emissions of the 2017 PNE fire (Yu et al., 2021). Wildfire smoke particles absorb solar energy and are self-lofted into the stratosphere. Simulations using CESM-CARMA (Yu et al., 2021) suggest that about two-thirds of the injected smoke particles mass (i.e., 0.9 Tg) at ~13 km rose into the lower and middle stratosphere during the first 2 months, and the remaining third was lost through transport and dry deposition out of the stratosphere or upper troposphere.

2.2. CESM-CARMA Aerosol Model

We use a sectional aerosol model, the Community Aerosol and Radiation Model for Atmospheres (CARMA), coupled with the Community Earth System Model (CESM-CARMA) (Bardeen et al., 2008; Toon et al., 1988; Yu et al., 2015), to simulate the volcanic and wildfire smoke aerosols in the upper troposphere and stratosphere. The model has 56 vertical layers from the surface up to 45 km with a vertical resolution of about 1 km in the upper troposphere and lower stratosphere (UTLS), and simulations are run on a grid of 1.9° latitude x 2.5° longitude. The model winds and temperatures are nudged to the ModernEra Retrospective Analysis for Research and Applications-2 (MERRA2) version of the Goddard Earth Observing System5 (GEOS-5) atmospheric general circulation model (AGCM) (Molod et al., 2015). The CESM-CARMA aerosol model tracks two groups of aerosols in 20 discrete size bins each: the first group is composed of pure sulfate and the other is composed of internal mixtures of various aerosol components including sulfate, organics, black carbon, dust, and salt. The radius of the pure sulfate particles ranges from 0.2 nm to 1.3 μm, and the radius of the mixed particles ranges from 0.05 to 8.7 μm (Yu et al., 2015).

CARMA calculates aerosol optical properties (extinction, absorption coefficients and single scattering albedo) for each particle size bin and 30 light wavelengths ranging from 0.23 to 55 μm. These optical properties are passed to the CESM1's radiation model (RRTMG) (Iacono et al., 2008) for online radiative calculation of forcing and heating rates. Details on the radiative coupling in CESM-CARMA is described in Yu et al. (2015).

We run the CESM-CARMA aerosol model from 2014 to 2022 with and without the volcanic and wildfire emissions. The difference between the two runs provides the aerosol anomalies due to these emissions. The wildfire

plume absorbs sunlight and rises rapidly from the troposphere to the stratosphere during the first 2 months (Kablick III et al., 2020; Khaykin et al., 2020; Yu et al., 2019, 2021). To simulate the self-rising of the wildfire smoke plume, the model is switched to the free-running mode for 2 months after the two pyroCb events start (i.e., the 2017 Pacific Northwest fire event, and the 2019–2020 Australian fire event). After 2 months for each wildfire event, we switch the model back to the nudging mode.

2.3. Balloon-Borne Optical Particle Spectrometers

Portable optical particle spectrometers (POPS) are lightweight and low power-consumption, which makes them easily deployable on weather balloons (Gao et al., 2016; Todt et al., 2023). Each particle passing through the laser beam creates a signal, which is used to calculate particle size assuming a spherical shape and an index of refraction. POPS counts particles between 70 nm and 1.25 μm in radius.

2.4. Estimation of Global Mean Surface Temperature (GMST) From ERF

The ERF is calculated within the climate model using fixed sea surface temperature (Hansen et al., 2005). The GMST response to the moderate volcanic and wildfire events is expected to be small compared with variability and thus difficult to diagnose by the climate model with a coupled ocean. Therefore, we estimate the change of GMST in response to the stratospheric ERF due to volcanic and wildfire events based on the temporal kernel method developed by Good et al. (2011). The GMST kernel time series is from the abrupt step-change experiment ($4\times\text{CO}_2$) from CMIP5 models. The GMST mean kernel is derived from 27 CMIP5 models, which are fit with the function presented in Equation 7 of Larson and Portmann (2016). The GMST anomaly is then derived using Equation 1 of Good et al. (2011).

3. Results

3.1. Stratospheric Injections Between 2014 and 2022

Aerosol surface area density (SAD) is one of the key parameters to quantify the heterogeneous reaction rates and radiative effects of stratospheric aerosols. Long-term in-situ observations of SAD are available from balloon-borne POPS (Gao et al., 2016) launched in Boulder, Colorado (40°N , 105°W), and in cities on the Tibetan Plateau including Lhasa (30°N , 91°E), Golmud (36.4°N , 94.9°E), and Kunming (25°N , 102°E). As shown in Figures 1a and 1b, the simulated and observed background SAD averaged between 30°N and 40°N are about $1\ \mu\text{m}^2/\text{cm}^3$ and $2\ \mu\text{m}^2/\text{cm}^3$ at 18.5 km (lower stratosphere) and 15.5 km (upper troposphere), respectively. Simulated SAD at 15.5 km is elevated in summer each year due to aerosol enhancement near the tropopause over the Tibetan Plateau, associated with the Asian summer monsoon (Vernier et al., 2015; Yu et al., 2017). Simulated SAD in the Northern Hemisphere (NH) mid-latitudes is significantly perturbed after 2017 at both altitudes, while significant SAD anomalies at lower altitudes in the upper troposphere are simulated before 2017. This indicates that the volcanic plumes in NH and tropics after 2017 reach higher altitudes than those of events between 2014 and 2017. Figure S1 in Supporting Information S1 compares the observed satellite and simulated aerosol extinction coefficients at mid-visible wavelengths from 2014 to 2021 at multiple altitudes. A substantial increase in the aerosol extinction is found in both model simulations and satellites data after volcanic eruptions (e.g., Kelut 2014, Calbuco 2015, Ambae 2018 and Taal 2020), as well as after the Australian wildfire in 2019–2020. Simulated SAD anomalies at 100 mb are elevated in both hemispheres, with larger perturbation in the SH (Figure S2A in Supporting Information S1). The 2015 Calbuco eruption and the 2019–2020 Australian wildfire each contribute about 10% of the simulated global mean SAD anomalies between 2014 and 2022, with 80% contributed mostly by other volcanic eruptions (Figure S2B in Supporting Information S1). Shown in Figure 1, POPS launched in July–December of 2019 in Boulder measured a large enhancement of SAD at 18 km inside of the Raikoke plume (Todt et al., 2023). Neither the model simulations (Figure 1) nor the satellite data (Figure S1 in Supporting Information S1) captured the large enhancement. It is difficult for climate models and satellites with relatively coarse sampling resolutions to capture the localized plumes.

The total injected SO_2 and wildfire biomass burning aerosol mass in the two 8-year periods (2005–2013 and 2014–2022) was roughly one-third of those between 1991 and 1999. From 2014 to 2022, 1.5 Tg of the total 4 Tg ($\sim 38\%$) was injected above 20 km and at low and mid-latitudes in the upwelling region of Brewer Dobson

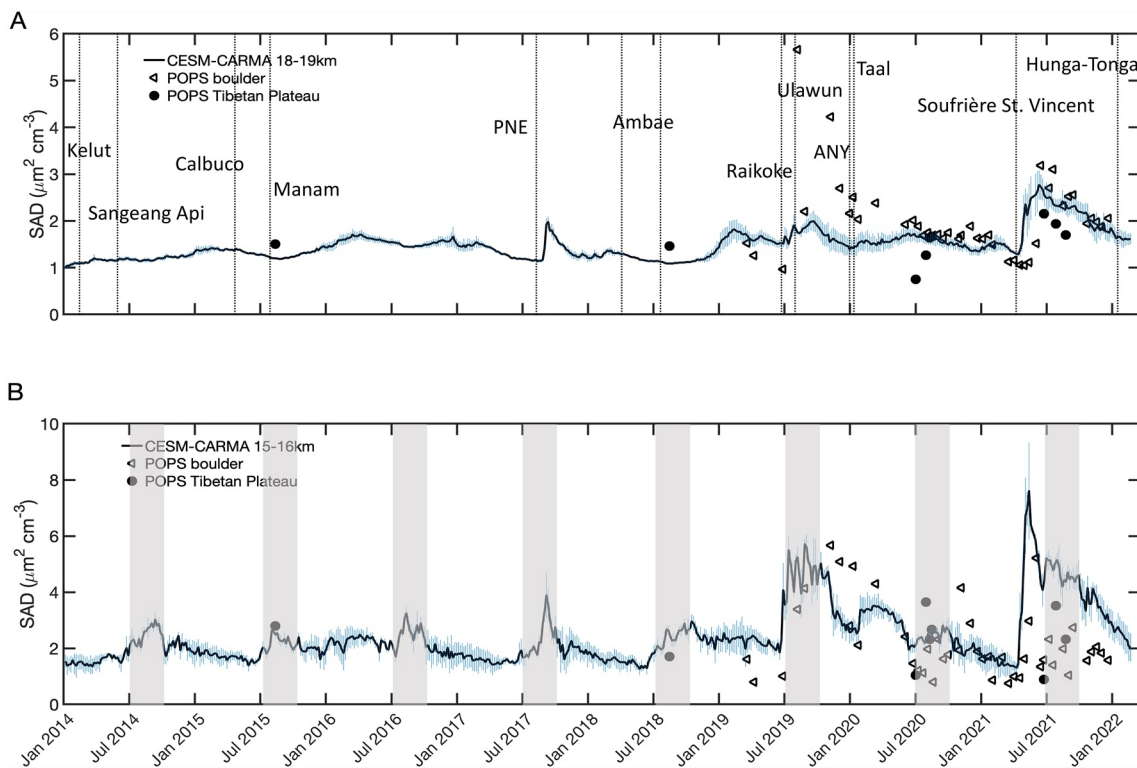


Figure 1. (a) Simulated aerosol surface area density (SAD) at 18.5 km from 2014 to 2022 averaged between 30°N and 40°N is denoted by solid lines. Error bars denote the latitudinal variability (one standard deviation) of the modeled SAD. Observations from portable optical particle spectrometers (POPS) launched in Boulder, Colorado, and the Tibetan Plateau (TP) are denoted by the open triangles and filled circles, respectively; Selected volcanic and wildfire events with the emission greater than 0.3 Tg are marked; (b) same as (a) but for altitude of 15.5 km. The gray shadings denote the seasons of Asian summer monsoon (July-August-September).

circulation (BDC) (Figure 2). In contrast, ~74% of the volcanic SO₂ between 2005 and 2013 was injected at 12–17 km in NH mid- to high-latitudes, where sulfate aerosols are subject to fast sedimentation and poleward and downward transport through the BDC. Consequently, the simulated aerosol optical depth anomaly and aerosol lifetime in 2014–2022 is ~50% higher than those in 2005–2013 (Table S2 in Supporting Information S1). In the lower stratosphere, the simulated SAD anomalies in the two 8-year periods are distributed in different hemispheres (Figure 2). The SAD anomalies in the lower stratosphere between 2014 and 2022 occur predominantly in the tropics and SH middle and high latitudes, which can influence the Antarctic lower stratospheric ozone budget, while the 2005–2013 anomalies are at NH mid-high latitudes.

3.2. Effective Radiative Forcing Between 2014 and 2022

Effective radiative forcing (ERF) at the top of the atmosphere (TOA) is a climate metric which considers rapid adjustments to atmospheric temperature changes (Larson & Portmann, 2016). A previous study (Hansen et al., 2005) reported a linear relationship between the global stratospheric AOD (sAOD) anomaly at mid-visible and the global mean ERF at TOA with a slope (Ω) of -23 W m^{-2} per unit sAOD anomaly (range from -21 to -30). Our estimated slope (Ω) is -22.5 W m^{-2} per unit sAOD anomaly averaged between 1991.6 and 1992.6 following the Pinatubo eruption. A similar slope was found in previous studies (Larson & Portmann, 2016; A. Schmidt et al., 2018). The calculated ERF between simulations with and without emissions is -0.11 W m^{-2} for the period of 2005–2013 and -0.45 W m^{-2} for the period of 1991–1999, respectively (Figure 3).

Tropospheric black carbon warms the atmosphere, resulting in a positive ERF at TOA, while stratospheric black carbon cools the atmosphere, resulting in a negative ERF (Ban-Weiss et al., 2012; Yu et al., 2016). A large amount of the ERF is in the rapid longwave (LW) adjustment term for a stratospheric warming agent (Shine et al., 2022). The calculated slopes (Ω) are around -37 W m^{-2} per unit sAOD change in one simulation of the ANY wildfire smoke and another sensitivity simulation with half of the ANY smoke emission (half-ANY). A similar slope

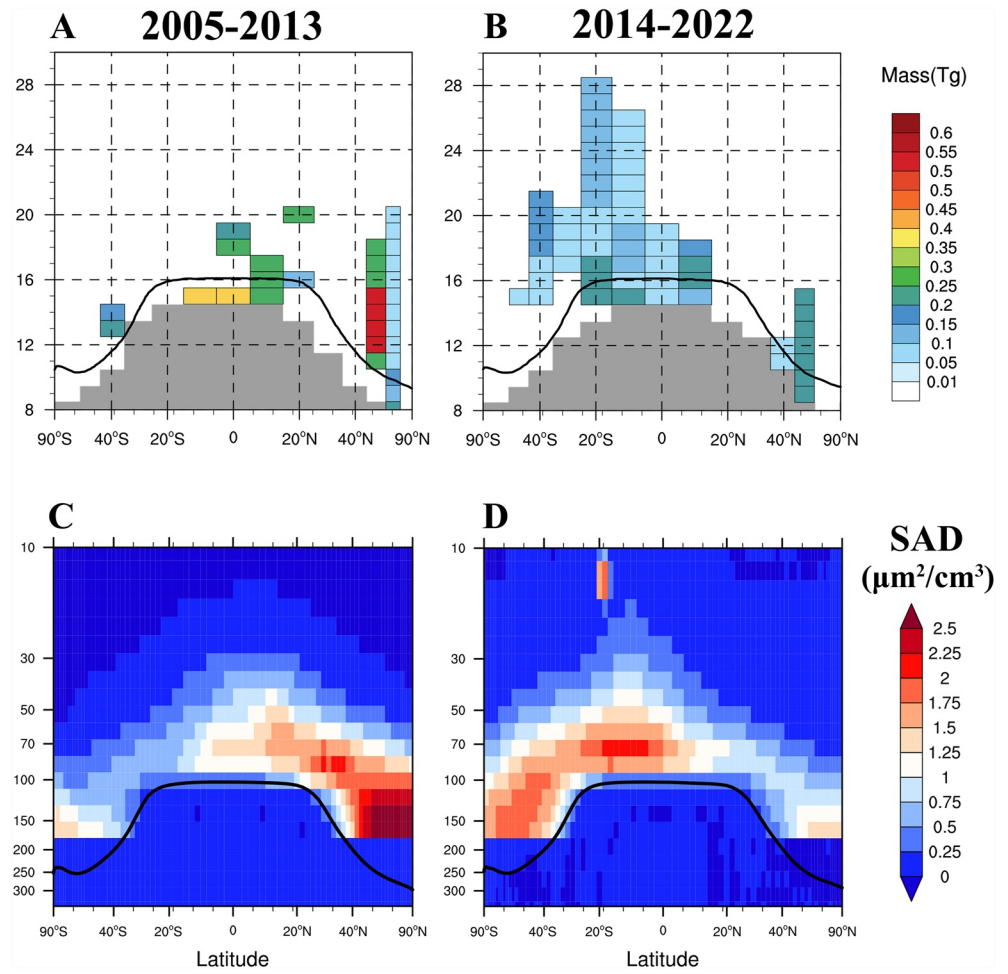


Figure 2. (a) Latitudinal and vertical distribution of the volcanic injected mass from the upper troposphere (2 km below the tropopause) to 30 km between 2005 and 2013; (b) same as (a) but for the injected mass from the volcanic and wildfire events between 2014 and 2022; (c) Simulated multi-annual and zonal averaged SAD anomalies due to volcanic injections from 2005 to 2013; (d) same as (c) but for volcanic and pyroCb SAD anomalies from 2014 to 2022.

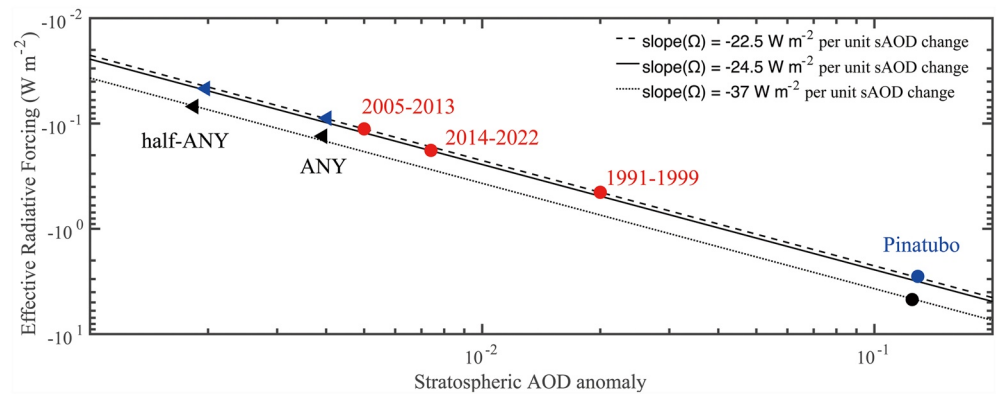


Figure 3. Calculated global mean ERF ($W m^{-2}$) at the TOA for 2005–2013, 2014–2022, and 1991–1999. The black lines denote the relationship between ERF and sAOD with a slope (Ω) of -22.5 , -24.5 and $-37 W m^{-2}$ per sAOD, respectively. The annual and global mean ERF and sAOD anomalies for the ANY wildfire and one sensitivity simulation with 50% of ANY smoke emission are shown by the black triangles. The simulated ERF with smoke replaced by sulfate is denoted by the blue triangles respectively. The ERF and sAOD anomalies for the first year of 1991 Pinatubo eruption is denoted by the blue circle. The simulated ERF with Pinatubo emissions replaced by smoke is denoted by the black circle.

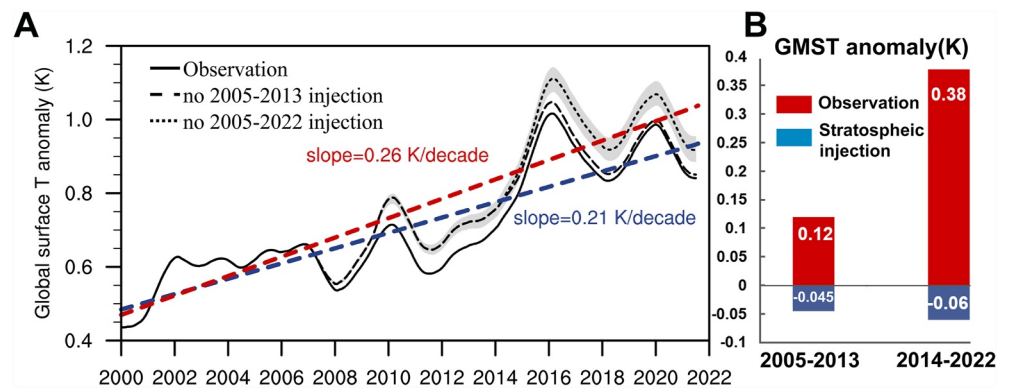


Figure 4. (a) Observed global and annual mean surface temperature anomaly from 2000 to 2022 relative to the average temperature between 1901 and 2000 (black line). The black dashed line denotes the temperature anomaly without 2005–2013 stratospheric injections. The black dotted line represents the temperature anomaly without 2005–2022 stratospheric injections. The gray shading denotes one standard deviation from the choice of CMIP5 GMST kernels. The red and blue dashed lines represent the linear fit with and without stratospheric injections, respectively; (b) Observed GMST anomalies of 2005–2013 and 2014–2022 relative to that in 1999–2002 (red bars). The simulated GMST anomalies of 2005–2013 and 2014–2022 due to the stratospheric injections.

(Ω) is found when we replace the 1991 Mt. Pinatubo emission with the smoke emissions (Figure 3). When we replace the smoke with sulfate in the ANY and half-ANY simulations instead, a less negative slope (Ω) of about -22.5 W m^{-2} per unit sAOD anomaly is simulated. Volcanic sulfate aerosol primarily scatters visible light with a portion of light scattered forward. Smoke particles absorb solar energy, thereby reducing the amount that reaches the troposphere. Absorption generates more negative instantaneous radiative forcing at the tropopause and surface than scattering. In addition, the temperature-adjusted stratosphere in response to smoke particles' absorption and heating emits LW radiation back to space and generates more negative ERF at TOA than volcanic sulfate aerosol. The positive change in the shortwave (SW) forcing at TOA (i.e., less outgoing SW) is overcome by the negative change of the LW radiative forcing (i.e., more outgoing LW) when we replace Mt. Pinatubo sulfur emission with the wildfire smoke (Figure 3; Table S3 in Supporting Information S1). The opposite changes occur when we replace ANY smoke emission with sulfate. Our study suggests that the stratospheric wildfire smoke absorbs the solar radiation, warms the stratosphere, and produces about 60% more negative ERF at the TOA per unit sAOD change than volcanic aerosols. Our study underscores that studies which fail to separate wildfire smoke from the volcanic sulfate might underestimate the negative stratospheric forcings in a warming climate.

The simulated mean sAOD anomaly is 0.0074 for the 2014–2022 period with $\sim 10\%$ of that contributed by the wildfire smoke. Assuming the stratospheric smoke ($\Omega = -37$) and volcanic sulfate ($\Omega = -22.5$) are independent in terms of the radiative properties, the estimated 8-year averaged ERF from 2014 to 2022 is -0.18 W m^{-2} . Note, the 1991 Mt. Pinatubo eruption represents the largest event in terms of mass of SO_2 emitted in the satellite era. The simulated ERF from the moderate volcanic and wildfire events in the period of 2014–2022 is $\sim 40\%$ of the period of 1991–1999. The carbon dioxide (CO_2) forcing increased by about 0.52 W m^{-2} from the volcanic quiescent period of 1999–2002 to 2014–2022; the estimated stratospheric volcanic ERF of 1999–2002 is -0.04 W m^{-2} (A. Schmidt et al., 2018); therefore, the estimated change in stratospheric volcanic and wildfire ERF between the same two periods is -0.14 W m^{-2} , which offsets about 26% of the increase in CO_2 forcing from 1999–2002 to 2014–2022.

4. Discussions

Volcanic eruptions were suggested to have contributed to the slowing of the rate of change in the global mean surface temperature (GMST) during the so called “hiatus” between 2000 and 2013 with a mean volcanic ERF of -0.1 W m^{-2} (A. Schmidt et al., 2018). Our study shows that the volcanic and wildfire activities during 2014–2022 generates 80% more ERF than the “hiatus” period. Figure 4a shows that the observed GMST of 2014–2022 increased by 0.38 K relative to the volcanic quiescent period (1999–2002) (<https://www.ncdc.noaa.gov/cag/>). GMST anomaly of 2014–2022 is a convolution of responses to all previous forcing changes including greenhouse gases, stratospheric and tropospheric aerosols, ocean heat content and internal variability. Based on a simple step response model (Good et al., 2011) with the mean kernel of GMST derived from the 5th Climate Model

Intercomparison Project (CMIP5), the 2014–2022 and 2005–2013 stratospheric injections decreased the GMST of 2014–2022 by 0.06 and 0.02 K, respectively (Figure 4a). The total offsets ~20% of the observed GMST anomaly of 2014–2022 relative to 1999–2002. The increase rate of GMST from 2000 to 2022 would have been ~24% larger without the stratospheric injections after 2005. This simple method of computing GMST changes brings large uncertainties like the choice of GMST kernels (see Larson & Portmann, 2016).

The estimated ERF is 80% larger in 2014–2022 than in 2005–2013 because the 2014–2022 emissions were injected at higher altitudes and lower latitudes and smoke provided more negative ERF than sulfate. Our study suggests that the stratospheric injections of 2014–2022 offset about 15% of the observed GMST increase between 2014–2022 and 1999–2002, while the 2005–2013 injections offset 38% of the observed GMST increase between 2005–2013 and 1999–2002 (Figure 4b). This reduced fractional impact of the aerosols on GMST, despite their larger ERF in 2014–2022, is due to the rapid increase in greenhouse gas forcing over the time periods considered. In the not-too-distant future, aerosols forcing of climate will no longer be competitive with greenhouse gas forcing and will no longer offset a significant portion of it.

5. Summary

We performed numerical simulations of the stratospheric volcanic and wildfire events between year 2014 and 2022. Simulated stratospheric aerosol surface area density (SAD) is compared against long-term in-situ observations from balloon-borne POPS (Gao et al., 2016; Todt et al., 2023) launched in Boulder, Colorado (40°N, 105°W), and in cities on the Tibetan Plateau. Both model and POPS suggest that the SAD in the Northern Hemispheric mid-latitudes is around 1–2 $\mu\text{m}^2/\text{cm}^3$ in the upper troposphere and lower stratosphere (15.5–18.5 km). The model captures the SAD enhancement and transport from the major volcanic and wildfire events, and suggests that the 2019–2020 Australian wildfire event and 2015 Calbuco eruption each contribute to about 10% of the simulated SAD anomalies between 2014 and 2022. Compared with the period of 2005–2013, stratospheric aerosols between 2014 and 2022 are injected at higher altitudes and lower latitudes with about 50% longer lifetime. Consequently, the simulated ERF change of the 2014–2022 injections is 80% more negative than the period of 2005–2013.

Wildfire organics and black carbon aerosols warm the stratosphere and produced more outgoing long-wave radiation to the space through stratospheric fast temperature adjustment (Shine et al., 2022). Our model simulations suggest that the effective radiative forcing (ERF) of stratospheric wildfire smoke is -37 W m^{-2} per unit change of stratospheric aerosol optical depth (sAOD), which is about 60% more negative than the volcanic sulfate. Our study underscores that studies which fail to separate wildfire smoke from the volcanic sulfate might underestimate the negative stratospheric forcings in a warming climate.

Our study shows that the stratospheric aerosol slows down the rate of global warming: it offsets about 26% of the increase in ERF and about 20% of the increase in GMST due to CO_2 from 1999–2002 to 2014–2022. Due to the rapid increase in greenhouse gas forcing, aerosol negative radiative forcing will no longer offset a significant portion of it. The contribution of extreme wildfire and moderate volcanic activities to the global radiation budget in the warming climate merits further study.

Data Availability Statement

The stratospheric aerosol surface area density data and model simulations are located at <https://doi.org/10.17605/OSF.IO/KBAFU>. OMPS-LP data are publicly available at <https://ozoneaq.gsfc.nasa.gov/data/ozone/>.

References

- Ban-Weiss, G. A., Cao, L., Bala, G., & Caldeira, K. (2012). Dependence of climate forcing and response on the altitude of black carbon aerosols. *Climate Dynamics*, 38(5), 897–911. <https://doi.org/10.1007/s00382-011-1052-y>
- Bardeen, C. G., Toon, O. B., Jensen, E. J., Marsh, D. R., & Harvey, V. L. (2008). Numerical simulations of the three-dimensional distribution of meteoric dust in the mesosphere and upper stratosphere. *Journal of Geophysical Research*, 113(D17), D17202. <https://doi.org/10.1029/2007JD009515>
- Bernath, P., Boone, C., & Crouse, J. (2022). Wildfire smoke destroys stratospheric ozone. *Science*, 375(6586), 1292–1295. <https://doi.org/10.1126/science.abm5611>
- Gao, R. S., Telg, H., McLaughlin, R. J., Ciciora, S. J., Watts, L. A., Richardson, M. S., et al. (2016). A light-weight, high-sensitivity particle spectrometer for PM_{2.5} aerosol measurements. *Aerosol Science and Technology*, 50(1), 88–99. <https://doi.org/10.1080/02786826.2015.1131809>

Acknowledgments

The CESM project is supported by the National Science Foundation and the Office of Science (BER) of the U.S. Department of Energy. We acknowledge high-performance computing support from Cheyenne (<https://doi.org/10.5065/D6RX99HX>) provided by NCAR's Computational and Information Systems Laboratory, sponsored by the National Science Foundation. This work is supported by the second Tibetan Plateau Scientific Expedition and Research Program (STEP, 2019QZKK0604) and the National Natural Science Foundation of China (42121004, 42175089).

- Good, P., Gregory, J. M., & Lowe, J. A. (2011). A step-response simple climate model to reconstruct and interpret AOGCM projections: A step-response simple climate model. *Geophysical Research Letters*, 38(1), L01703. <https://doi.org/10.1029/2010GL045208>
- Hansen, J., Sato, M., Ruedy, R., Nazarenko, L., Lacis, A., Schmidt, G. A., et al. (2005). Efficacy of climate forcings. *Journal of Geophysical Research*, 110(D18), D18104. <https://doi.org/10.1029/2005JD005776>
- Iacono, M. J., Delamere, J. S., Mlawer, E. J., Shephard, M. W., Clough, S. A., & Collins, W. D. (2008). Radiative forcing by long-lived greenhouse gases: Calculations with the AER radiative transfer models. *Journal of Geophysical Research*, 113(D13), D13103. <https://doi.org/10.1029/2008JD009944>
- Ivy, D. J., Solomon, S., Kinnison, D., Mills, M. J., Schmidt, A., & Neely, R. R., III. (2017). The influence of the Calbuco eruption on the 2015 Antarctic ozone hole in a fully coupled chemistry-climate model. *Geophysical Research Letters*, 44(5), 2556–2561. <https://doi.org/10.1002/2016GL071925>
- Kablick, G. P., III, Allen, D. R., Fromm, M. D., & Nedoluha, G. E. (2020). Australian PyroCb smoke generates synoptic-scale stratospheric anticyclones. *Geophysical Research Letters*, 47(13), e2020GL088101. <https://doi.org/10.1029/2020GL088101>
- Khaykin, S., Legras, B., Bucci, S., Sellitto, P., Isaksen, I., Tencé, F., et al. (2020). The 2019/20 Australian wildfires generated a persistent smoke-charged vortex rising up to 35 km altitude. *Communications Earth & Environment*, 1(1), 1–12. <https://doi.org/10.1038/s43247-020-00022-5>
- Larson, E. J. L., & Portmann, R. W. (2016). A temporal kernel method to compute effective radiative forcing in CMIP5 transient simulations. *Journal of Climate*, 29(4), 1497–1509. <https://doi.org/10.1175/JCLI-D-15-0577.1>
- Mills, M. J., Schmidt, A., Easter, R., Solomon, S., Kinnison, D. E., Ghan, S. J., et al. (2016). Global volcanic aerosol properties derived from emissions, 1990–2014, using CESM1(WACCM). *Journal of Geophysical Research: Atmospheres*, 121(5), 2332–2348. <https://doi.org/10.1002/2015JD024290>
- Molod, A., Takacs, L., Suarez, M., & Bacmeister, J. (2015). Development of the GEOS-5 atmospheric general circulation model: Evolution from MERRA to MERRA2. *Geoscientific Model Development*, 8(5), 1339–1356. <https://doi.org/10.5194/gmd-8-1339-2015>
- Neely, R. R., III, & Schmidt, A. (2016). VolcanEESM: Global volcanic sulphur dioxide (SO₂) emissions database from 1850 to present.
- Rieger, L. A., Randel, W. J., Bourassa, A. E., & Solomon, S. (2021). Stratospheric temperature and ozone anomalies associated with the 2020 Australian new year fires. *Geophysical Research Letters*, 48(24), e2021GL095898. <https://doi.org/10.1029/2021GL095898>
- Santee, M. L., Lambert, A., Manney, G. L., Livesey, N. J., Froidevaux, L., Neu, J. L., et al. (2022). Prolonged and pervasive perturbations in the composition of the southern hemisphere midlatitude lower stratosphere from the Australian new year's fires. *Geophysical Research Letters*, 49(4), e2021GL096270. <https://doi.org/10.1029/2021GL096270>
- Santer, B. D., Bonfils, C., Painter, J. F., Zelinka, M. D., Mears, C., Solomon, S., et al. (2014). Volcanic contribution to decadal changes in tropospheric temperature. *Nature Geoscience*, 7(3), 185–189. <https://doi.org/10.1038/ngeo2098>
- Schmidt, A., Mills, M. J., Ghan, S., Gregory, J. M., Allan, R. P., Andrews, T., et al. (2018). Volcanic radiative forcing from 1979 to 2015. *Journal of Geophysical Research: Atmospheres*, 123(22), 12491–12508. <https://doi.org/10.1029/2018JD028776>
- Schmidt, G. A., Shindell, D. T., & Tsigaridis, K. (2014). Reconciling warming trends. *Nature Geoscience*, 7(3), 158–160. <https://doi.org/10.1038/ngeo2105>
- Shine, K. P., Byrom, R. E., & Checa-Garcia, R. (2022). Separating the shortwave and longwave components of greenhouse gas radiative forcing. *Atmospheric Science Letters*, 23(10), e1116. <https://doi.org/10.1002/asl.1116>
- Solomon, S. (1999). Stratospheric ozone depletion: A review of concepts and history. *Reviews of Geophysics*, 37(3), 275–316. <https://doi.org/10.1029/1999RG900008>
- Solomon, S., Daniel, J. S., Neely, R. R., Vernier, J.-P., Dutton, E. G., & Thomason, L. W. (2011). The persistently variable “background” stratospheric aerosol layer and global climate change. *Science*, 333(6044), 866–870. <https://doi.org/10.1126/science.1206027>
- Solomon, S., Dube, K., Stone, K., Yu, P., Kinnison, D., Toon, O. B., et al. (2022). On the stratospheric chemistry of midlatitude wildfire smoke. *Proceedings of the National Academy of Sciences*, 119(10), e2117325119. <https://doi.org/10.1073/pnas.2117325119>
- Solomon, S., Ivy, D. J., Kinnison, D., Mills, M. J., Neely, R. R., & Schmidt, A. (2016). Emergence of healing in the Antarctic ozone layer. *Science*, 353(6296), 269–274. <https://doi.org/10.1126/science.aae0061>
- Solomon, S., Stone, K., Yu, P., Murphy, D. M., Kinnison, D., Ravishankara, A. R., & Wang, P. (2023). Chemical impacts of wildfire smoke on stratospheric chlorine and ozone depletion. *Nature*, 615(7951), 259–264. <https://doi.org/10.1038/s41586-022-05683-0>
- Stone, K. A., Solomon, S., Kinnison, D. E., Pitts, M. C., Poole, L. R., Mills, M. J., et al. (2017). Observing the impact of Calbuco volcanic aerosols on south polar ozone depletion in 2015. *Journal of Geophysical Research: Atmospheres*, 122(21), 11862–11879. <https://doi.org/10.1002/2017JD026987>
- Todt, M. A., Asher, E., Hall, E., Cullis, P., Jordan, A., Xiong, K., et al. (2023). Baseline Balloon Stratospheric Aerosol Profiles (B2SAP)—Systematic measurements of aerosol number density and size. *Journal of Geophysical Research: Atmospheres*, 128, e2022JD038041. <https://doi.org/10.1029/2022JD038041>
- Toon, O. B., Turco, R. P., Westphal, D., Malone, R., & Liu, M. (1988). A multidimensional model for aerosols: Description of computational analogs. *Journal of the Atmospheric Sciences*, 45(15), 2123–2144. [https://doi.org/10.1175/1520-0469\(1988\)045<2123:AMMFAD>2.0.CO;2](https://doi.org/10.1175/1520-0469(1988)045<2123:AMMFAD>2.0.CO;2)
- Vernier, J.-P., Fairlie, T. D., Natarajan, M., Wienhold, F. G., Bian, J., Martinsson, B. G., et al. (2015). Increase in upper tropospheric and lower stratospheric aerosol levels and its potential connection with Asian pollution. *Journal of Geophysical Research: Atmospheres*, 120(4), 1608–1619. <https://doi.org/10.1002/2014JD022372>
- Yu, P., Davis, S. M., Toon, O. B., Portmann, R. W., Bardeen, C. G., Barnes, J. E., et al. (2021). Persistent stratospheric warming due to 2019–2020 Australian wildfire smoke. *Geophysical Research Letters*, 48(7), e2021GL092609. <https://doi.org/10.1029/2021GL092609>
- Yu, P., Murphy, D. M., Portmann, R. W., Toon, O. B., Froyd, K. D., Rollins, A. W., et al. (2016). Radiative forcing from anthropogenic sulfur and organic emissions reaching the stratosphere. *Geophysical Research Letters*, 43(17), 9361–9367. <https://doi.org/10.1002/2016GL070153>
- Yu, P., Rosenlof, K. H., Liu, S., Telg, H., Thornberry, T. D., Rollins, A. W., et al. (2017). Efficient transport of tropospheric aerosol into the stratosphere via the Asian summer monsoon anticyclone. *Proceedings of the National Academy of Sciences of the United States of America*, 114(27), 6972–6977. <https://doi.org/10.1073/pnas.1701170114>
- Yu, P., Toon, O. B., Bardeen, C. G., Mills, M. J., Fan, T., English, J. M., & Neely, R. R. (2015). Evaluations of tropospheric aerosol properties simulated by the community Earth system model with a sectional aerosol microphysics scheme. *Journal of Advances in Modeling Earth Systems*, 7(2), 865–914. <https://doi.org/10.1002/2014MS000421>
- Yu, P., Toon, O. B., Bardeen, C. G., Zhu, Y., Rosenlof, K. H., Portmann, R. W., et al. (2019). Black carbon lofts wildfire smoke high into the stratosphere to form a persistent plume. *Science*, 365(6453), 587–590. <https://doi.org/10.1126/science.aax1748>
- Zhu, Y., Toon, O. B., Kinnison, D., Harvey, V. L., Mills, M. J., Bardeen, C. G., et al. (2018). Stratospheric aerosols, polar stratospheric clouds, and polar ozone depletion after the Mount Calbuco eruption in 2015. *Journal of Geophysical Research: Atmospheres*, 123(21), 12308–12331. <https://doi.org/10.1029/2018JD028974>